

# Flagellar phenotypic plasticity in volvocalean algae correlates with Péclet number

Cristian A. Solarí<sup>1</sup>, Knut Drescher<sup>2</sup>, Sujoy Ganguly<sup>2</sup>,  
John O. Kessler<sup>3</sup>, Richard E. Michod<sup>4</sup> and Raymond E. Goldstein<sup>2,\*</sup>

<sup>1</sup>CONICET, Laboratorio de Biología Comparada de Protistas, Departamento de Biodiversidad y Biología Experimental (FCEN), Universidad de Buenos Aires, C1428EHA Buenos Aires, Argentina

<sup>2</sup>Department of Applied Mathematics and Theoretical Physics, Centre for Mathematical Sciences, University of Cambridge, Wilberforce Road, Cambridge CB3 0WA, UK

<sup>3</sup>Department of Physics, and <sup>4</sup>Department of Ecology and Evolutionary Biology, University of Arizona, Tucson, AZ 85721, USA

Flagella-generated fluid stirring has been suggested to enhance nutrient uptake for sufficiently large micro-organisms, and to have played a role in evolutionary transitions to multicellularity. A corollary to this predicted size-dependent benefit is a propensity for phenotypic plasticity in the flow-generating mechanism to appear in large species under nutrient deprivation. We examined four species of volvocalean algae whose radii and flow speeds differ greatly, with Péclet numbers ( $Pe$ ) separated by several orders of magnitude. Populations of unicellular *Chlamydomonas reinhardtii* and one- to eight-celled *Gonium pectorale* ( $Pe \sim 0.1$ – $1$ ) and multicellular *Volvox carteri* and *Volvox barberi* ( $Pe \sim 100$ ) were grown in diluted and undiluted media. For *C. reinhardtii* and *G. pectorale*, decreasing the nutrient concentration resulted in smaller cells, but had no effect on flagellar length and propulsion force. In contrast, these conditions induced *Volvox* colonies to grow larger and increase their flagellar length, separating the somatic cells further. Detailed studies on *V. carteri* found that the opposing effects of increasing beating force and flagellar spacing balance, so the fluid speed across the colony surface remains unchanged between nutrient conditions. These results lend further support to the hypothesized link between the Péclet number, nutrient uptake and the evolution of biological complexity in the Volvocales.

**Keywords:** phenotypic plasticity; evolution; *Volvox*; flagella; fluid dynamics; nutrient uptake

## 1. INTRODUCTION

A fundamental subject in evolutionary biology is the evolutionary transition from unicellular organisms to multicellular ones, and the accompanying cellular differentiation and specialization [1,2]. Not surprisingly for micro-organisms living in an aqueous environment, many of the important factors are *physical*, involving diffusion and mixing, for the exchange of molecular species with the environment is one of the most basic factors of life. Progress on this important evolutionary issue therefore involves not only studies of molecular and genetic aspects of multicellular life, but also the introduction of techniques from transport theory to address the allometric scaling of metabolic activity with size [3].

At least since the work of Weismann [4], it has been recognized that a particularly interesting class of

organisms to study for insights into the origins of multicellularity is composed of the alga *Volvox* and its relatives. Volvocalean green algae are motile micro-organisms consisting of biflagellated cells. They range from the unicellular *Chlamydomonas* to colonies made of cells with no cellular differentiation, such as *Gonium* (one to eight cells), *Eudorina* (4–64 cells) and *Pleodorina* (16–256 cells), to the multicellular *Volvox* comprising 500–50 000 cells with specialization in reproductive and vegetative functions, i.e. germ–soma separation (figure 1; [6–8]). In the multicellular forms, each of the *Chlamydomonas*-like somatic cells is found at the surface of the extracellular matrix (ECM), with its two flagella oriented outwards, while the germ cells lose their flagella and grow on the inside of the colony (figure 1). The somatic cells may be connected through cytoplasmic bridges, as in *Volvox barberi*, or unconnected, as in *Volvox carteri*. Germ–soma separation in *Volvox* species such as *V. carteri* and *V. barberi* has evolved independently

\*Author for correspondence (r.e.goldstein@damtp.cam.ac.uk).

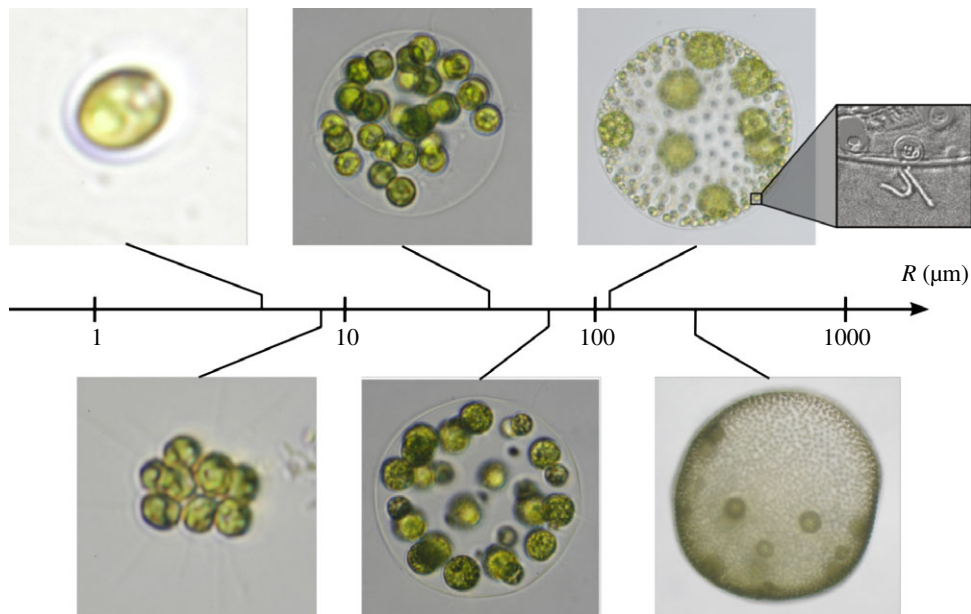


Figure 1. A selection of the volvoclean green algae, arranged according to organism radius  $R$  (after [5]). In order of increasing size, they are unicellular *C. reinhardtii*, undifferentiated *G. pectorale* and *Eudorina elegans*, followed by the soma-differentiated *Pleodorina californica* and germ–soma differentiated *V. carteri* and *V. barberi*. When two cell types can be recognized, the smaller are the somatic cells, the larger are the germ cells or daughter colonies.

from different ancestors [9–13]. In short, Volvocales comprise a group of closely related lineages with different degrees of cell specialization which seem to represent ‘alternative stable states’ [14] that reflect clearly the stages of the transition to multicellularity and cellular differentiation.

Volvocales are found in quiet, standing waters of transient vernal puddles or in permanent lakes when thermal stirring stops and the lake becomes stratified [6,15]. Because they are negatively buoyant, these organisms need flagellar beating to avoid sinking and to reach light and nutrients [7,8]. In addition to providing motility, flagella may also be important for generating advective flows that can increase nutrient uptake. If the Volvocales were to rely on diffusion alone to acquire nutrients from a quiescent fluid environment, the total rate of uptake would scale linearly with organism size. In contrast, the metabolic needs of Volvocales that form spheroids grow at least quadratically [5], implying that there is a bottleneck organism size beyond which diffusion alone is insufficient to feed the cells. This theoretical work, together with the empirical evidence given by Solari *et al.* [16], supports the idea that advective flows are important for enhancing nutrient uptake in the larger Volvocales. Changes in the flagellar apparatus between unicellular species and species that form colonies [17] also indicate that the demands on the flagella change with organism size. The emerging hypothesis is therefore that, for larger Volvocales, the collective beating of flagella not only yields motility, but also improves the molecular transport of nutrients, waste products and chemical messengers.

To quantify this hypothesis, we note that the Volvocales, along with most other micro-organisms, live in a world of Reynolds number  $Re \ll 1$  [18,19]. In this ‘Stokes flow’ regime, motion is dominated by viscosity,

fluid flows are linear and time reversible and nutrient transport is usually dominated by diffusion. However, on the surface of a *Volvox* colony, the collective beating of many closely spaced flagella can lead to fluid flows of sufficiently high speeds that nutrient transport by advection may replace diffusion as the most important mechanism. The relative importance of these transport processes can be quantified by first defining a typical fluid velocity  $U$ , length scale  $L$  and diffusion constant  $D$  ( $D \sim 2 \times 10^{-5} \text{ cm}^2 \text{ s}^{-1}$  for  $\text{O}_2$  is typical for small molecules). Then, a dimensionless ratio of the time scale for diffusion ( $t_{\text{diff}} = L^2/D$ ) and advection ( $t_{\text{adv}} = L/U$ ), known as the Péclet number ( $Pe = t_{\text{diff}}/t_{\text{adv}} = UL/D$ ), serves to characterize the relative importance of the two processes. If  $Pe < 1$ , diffusion is faster than the transport of molecules by advection via the flowing medium, indicating that an organism does not need to invest in flagellar beating to increase nutrient uptake. If however  $Pe > 1$ , advection through collectively generated flows may be important. For *Volvox* colonies, the flagellar beating leads to  $Pe \gg 1$ , while for the unicellular *Chlamydomonas*  $Pe \sim 0.1$  [16]. Self-generated flows (figure 2), produced by hundreds or thousands of somatic cells arrayed on the surface of *Volvox*, may thus free these large spherical colonies from the constraints of diffusion-limited nutrient uptake, facilitating the transition to multicellularity and germ–soma differentiation.

If the larger Volvocales have come to depend upon fluid flow generated by beating flagella for enhanced nutrient uptake, it stands to reason that conditions of nutrient deprivation might trigger changes in the motility apparatus to mitigate such an environmental stress. On the other hand, for much smaller organisms like *Chlamydomonas* and *Gonium*, such effects would not be expected. This type of response would be an example of phenotypic plasticity, defined as the production of multiple phenotypes from a single genotype, depending

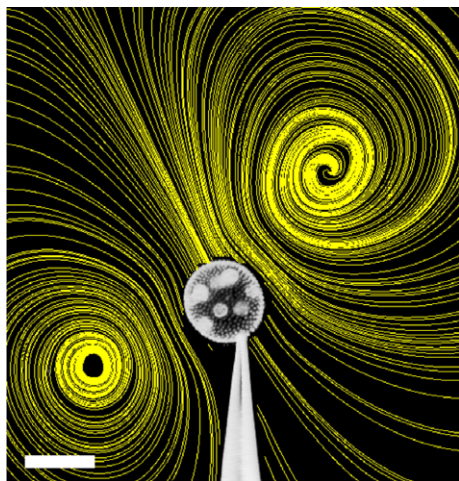


Figure 2. *Volvox carteri* held by a micropipette, with streamlines superimposed. Streamlines were obtained from a map of the flow field by particle imaging velocimetry. The flows, driven solely by the somatic cells' flagella at the surfaces of the colonies, extend outward by several colony diameters. The magnitude of the velocities near the colony can reach several hundred micrometres per second, and the regular, smooth flow from anterior to posterior can lead to enhanced acquisition and discharge of metabolites (as compared with diffusion in a quiescent environment), which is likely to be crucial for metabolism and productivity. Scale bar, 200  $\mu\text{m}$ .

on environmental conditions [20]. Phenotypic alterations in responses to biotic and abiotic factors have been well documented in a wide variety of organisms (e.g. for plants, see [20]). For example, when food is scarce, planktotrophic echinoderm larvae (plutei) produce longer food-gathering structures than when food is abundant [21].

Here we report evidence in favour of the hypothesis of Péclet-number-dependent phenotypic plasticity. This evidence was obtained by growing populations of four Volvocales species of very different size (*Chlamydomonas reinhardtii* and *Gonium pectorale* representing the low- $Pe$  species, and germ-soma differentiated *V. carteri* and *V. barberi* representing the high- $Pe$  species) in diluted and normal media. Standard microscopy and high-speed imaging were used to determine any phenotypic responses of the flagella and of the overall organism morphology. We found that the two *Volvox* species make an investment into increasing collective flagellar beating during nutrient deprivation, whereas under those same conditions *C. reinhardtii* and *G. pectorale* do not.

## 2. MATERIAL AND METHODS

Populations of *V. carteri* f. *nagariensis* EVE strain (kindly provided by D. L. Kirk), *V. barberi* (Carolina Supplies, cat. no. 152660), *C. reinhardtii* (UTEX 89) and *G. pectorale* (UTEX LB826) were synchronized in test tubes with 20 ml of standard *Volvox* medium (SVM; [22]), and illuminated by homogeneous cool white light [approx. 1000 foot candles; fc (1fc = 10.764 lux)] in a daily cycle of 16 h of light (at 28°C) and 8 h of darkness (at 26°C). Under these conditions, the asexual life cycle of *C. reinhardtii* and *G. pectorale*

has a 24 h generation time; cells grow during the light period, perform multiple divisions in the dark and daughter cells and colonies (for *Gonium*) are released when light returns. The asexual life cycle of *V. barberi* and *V. carteri* takes 48 h under these conditions, and is shown for *V. carteri* in figure 3.

To check for phenotypic plasticity, individuals were grown in two different nutrient concentrations as follows. From a synchronized population, just after individuals hatched (3, 6, 2 and 2 h into the light period for *V. carteri*, *V. barberi*, *C. reinhardtii* and *G. pectorale*, respectively), individuals were harvested by slow centrifugation, transferred to distilled water, centrifuged again and randomly separated into two sub-populations: one placed in full-strength SVM and the other in a  $10^{-1}$  dilution of SVM. For each species and for both nutrient treatments, the organism concentration was adjusted to approximately  $10^4$  cells  $\text{ml}^{-1}$ . The organism concentrations were therefore  $10^4$  *C. reinhardtii* cells  $\text{ml}^{-1}$ , approximately 1400 *G. pectorale* colonies  $\text{ml}^{-1}$  (colonies had on average seven cells), five *V. carteri* spheroids  $\text{ml}^{-1}$  (organisms had on average 2000 cells) and two *V. barberi* spheroids  $\text{ml}^{-1}$  (organisms had on average 5000 cells). Measurements were performed after the organisms were grown in the diluted and undiluted SVM for 8 h. During these 8 h, and the ensuing measurement period, all species were in their growth phase. During the experiments, cellular division did not take place in any species, except in *V. barberi*. In contrast to the other species, in which the reproductive cells grow about  $2^n$ -fold in size and then undergo a rapid series of  $n$  synchronous divisions (the 'palintomic' ancestral developmental programme), the reproductive cells of *V. barberi* have a derived developmental programme and perform binary fission to produce daughter colonies [13,23,24].

In all experiments, digital images were taken at high magnification and analysed with image processing software (METAMORPH, Universal Imaging Corp., PA, USA) to measure flagellar lengths, diameters of cells and *Volvox* spheroids and the number and diameter of reproductive and somatic cells. Cell and spheroid diameters were measured by taking the mean of two orthogonal diameters. The number of somatic cells per unit area on the surface of a *Volvox* spheroid was calculated by taking the mean somatic cell concentration from two opposite sides of the spheroid. A multiple linear regression (MLR) analysis was performed (JMP software; SAS Institute, Cary, NC, USA) using indicator variables to account for the nominal factors. Continuous variables were used to account for factors such as flagellar length and colony cell number.

### 2.1. Initial experiments on the phenotypic plasticity of the organism and flagellar sizes

Measurements were performed at two times ( $t_1$  and  $t_2$ ) in the life cycle of the organisms:  $t_1$  = just before the organisms were harvested (as detailed above), and  $t_2$  = 8 h later on the same day. For these measurements, Lugol solution was used to fix 1 ml samples of all organisms, except *V. barberi*. Samples of *V. barberi* were fixed



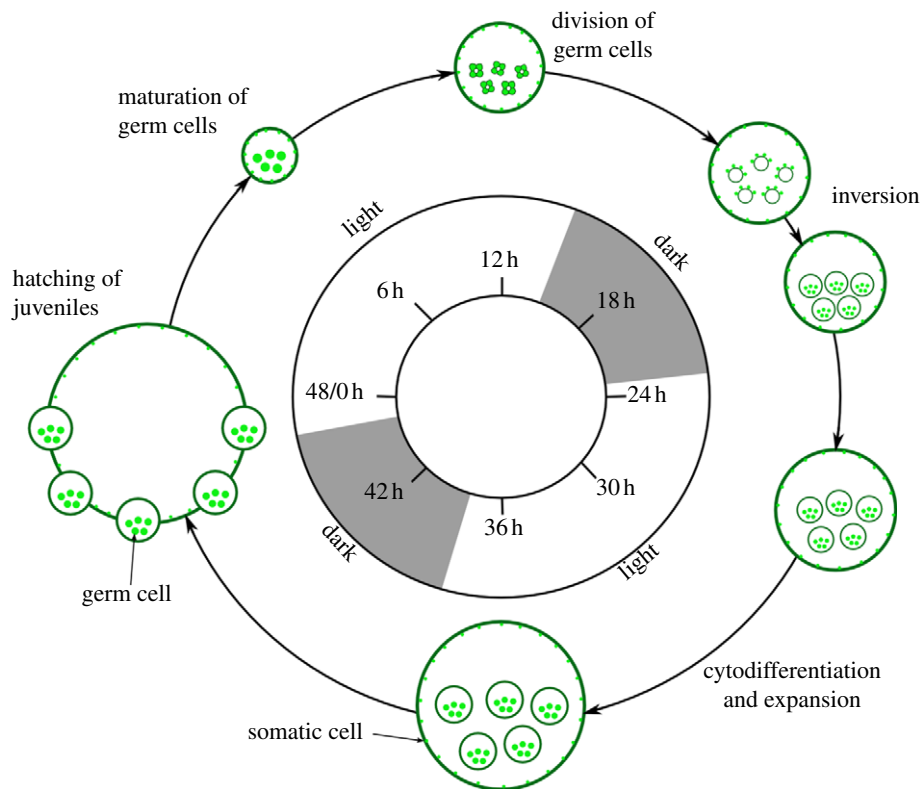


Figure 3. Life cycle of *V. carteri* (after [6]). When synchronized, *V. carteri* completes one asexual life cycle in 48 h. Colonies hatch 2 h into the light period and germ cells continue to grow until they begin multiple divisions towards the end of the light period. The divisions take approximately 7 h, and are followed by the inversion process that forms the daughter colonies inside the mother colony before the beginning of the next light period. The daughter colonies grow inside the mother colony for 24 h and hatch the next day.

with formalin instead of Lugol solution because the Lugol solution made their flagellar curl. Spheroid size, cell size and flagellar length were measured for 10 individuals for each nutrient treatment and species. For *G. pectorale*, measurements were averaged from two cells in each colony; for *Volvox* species, measurements were averaged on two germ cells and five somatic cells in each colony. The experiments were repeated three times, yielding for each species data on  $n = 30$  organisms at  $t_1$  and  $n = 60$  organisms between the two nutrient treatments at  $t_2$ .

## 2.2. Experiments for propulsion force measurement of *C. reinhardtii* and *G. pectorale*

To check for differences in propulsion force between the nutrient treatments, upward swimming  $V_{\text{up}}$  and sedimentation  $V_{\text{sed}}$  speeds were measured as detailed in Solari *et al.* [8] using the apparatus developed by Drescher *et al.* [25]. The growth conditions were as described in §2.1, but with a lower light intensity (approx. 600 fc) as the cultures for these experiments were grown in a different country and a different diurnal chamber that did not allow a higher light intensity. For each experiment, we measured  $V_{\text{up}}$  and  $V_{\text{sed}}$  of 30 individuals and the radius  $R$  of 15 individuals. As described in Solari *et al.* [8], the propulsion force  $F_p$  exerted by an individual swimming vertically upward at velocity  $V_{\text{up}}$  is balanced by the sum of the

drag force and gravity,  $F_p = 6\pi\eta R(V_{\text{up}} + V_{\text{sed}})$ . By using the population average of  $V_{\text{up}}$ ,  $V_{\text{sed}}$  and  $R$  in this equation, we obtain the population average of  $F_p$  for the two treatments. The experiments were repeated four times, yielding for each species data on  $n = 8$  populations between the two nutrient treatments at  $t_2$ .

## 2.3. Detailed experiments on the phenotypic plasticity of *V. carteri*

Flagellar lengths, beating frequencies and flagella-driven flow speeds of *V. carteri* were measured *in vivo*, while holding the spheroid in place by micropipette aspiration [16], as shown in figure 2. Spheroid sizes, cell sizes and flagellar lengths were measured as described in §2.1, but only at  $t_2$ . The growth conditions were as described in §2.1, but with a lower light intensity (approx. 600 fc) as in §2.2. Measurements were performed in the 2 h period beginning at  $t_2$ . This period was further divided into four sub periods of 30 min; in each sub period, measurements on five spheroids from the same nutrient treatment were performed, and the sub periods of measurements from each treatment were alternated (e.g. A/B/A/B or B/A/B/A). Flagella-driven flows around *V. carteri* were visualized with 1  $\mu\text{m}$  micro-spheres (Invitrogen Corp., CA, USA), recorded with a high-speed camera (Phantom v. 5.1, Vision Research, NJ, USA) and measured using particle image velocimetry (FlowManager, Dantec Dynamics, Skovlunde, Denmark). For the

Table 1. Data from populations grown at a light intensity of 1000 fc, i.e. experiment described in §2.1, in the format average  $\pm$  s.e. The number of organisms  $n$  that make up an average value is  $n=30$  in each case. The times  $t_1$  and  $t_2$  at which measurements were conducted are 1–2 h after hatching and 8 h later, respectively. The difference between treatments is given in absolute terms as the difference between the measurements in normal and diluted media at  $t_2$ , as obtained with an MLR model. The statistical  $p$ -value was obtained from the MLR model. A § marks statistically non-significant differences between treatments. Details of the MLR model used here are given in table 3. The symbols used are cell radius  $r_C$ , and flagellar length  $l$ , and *Volvox* spheroid radius  $R$ , germ cell radius  $r_G$ , somatic cell radius  $r_S$  and somatic cell concentration  $C$ . The average cell number of a *G. pectorale* colony was  $7.0 \pm 0.28$ . The average total number of somatic cells of a *V. carteri* colony was  $1970 \pm 56$ , and the average number of germ cells was  $11.9 \pm 0.2$ . The average total number of somatic cells of a *V. barberi* colony was  $4975 \pm 336$ , and the average number of germ cells was  $13.9 \pm 0.5$ .

	$t_1$ : normal medium	$t_2$ : normal medium	$t_2$ : diluted medium	difference between treatments		
				absolute	(%)	$p$ -value
<i>C. reinhardtii</i>						
$r_C$ ( $\mu\text{m}$ )	$3.43 \pm 0.07$	$5.24 \pm 0.20$	$4.73 \pm 0.16$	$-0.36 \pm 0.18$	$-6.9 \pm 3.4$	0.0431
$l$ ( $\mu\text{m}$ )	$10.4 \pm 0.33$	$9.07 \pm 0.40$	$9.11 \pm 0.34$	§	§	0.7362
<i>G. pectorale</i>						
$r_C$ ( $\mu\text{m}$ )	$4.66 \pm 0.11$	$5.51 \pm 0.15$	$5.03 \pm 0.16$	$-0.34 \pm 0.16$	$-6.2 \pm 2.9$	0.0204
$l$ ( $\mu\text{m}$ )	$17.17 \pm 1.29$	$17.75 \pm 0.67$	$19.06 \pm 0.49$	§	§	0.4140
<i>V. carteri</i>						
$R$ ( $\mu\text{m}$ )	$155 \pm 3.9$	$204 \pm 3.9$	$222 \pm 4.0$	$14.6 \pm 4.86$	$7.2 \pm 2.4$	0.0031
$r_G$ ( $\mu\text{m}$ )	$24.1 \pm 0.76$	$30.1 \pm 0.40$	$29.3 \pm 0.34$	$-1.16 \pm 0.63$	$-3.9 \pm 2.1$	0.0691
$r_S$ ( $\mu\text{m}$ )	$4.04 \pm 0.09$	$4.89 \pm 0.09$	$4.37 \pm 0.07$	$-0.46 \pm 0.09$	$-9.4 \pm 1.8$	<0.0001
$l$ ( $\mu\text{m}$ )	$14.9 \pm 0.71$	$18.2 \pm 0.50$	$20.45 \pm 0.46$	$2.14 \pm 0.68$	$11.7 \pm 3.7$	0.0021
$C$ (cells/ $10^3 \mu\text{m}^2$ )	$6.91 \pm 0.49$	$3.68 \pm 0.29$	$3.17 \pm 0.18$	$-0.65 \pm 0.33$	$-17.7 \pm 9.1$	0.0552
<i>V. barberi</i>						
$R$ ( $\mu\text{m}$ )	$217 \pm 5.4$	$279 \pm 12.4$	$326 \pm 7.2$	$59.1 \pm 11.0$	$21.1 \pm 3.9$	<0.0001
$r_G$ ( $\mu\text{m}$ )	$14.0 \pm 1.17$	$27.3 \pm 1.21$	$29.7 \pm 1.68$	§	§	
$r_S$ ( $\mu\text{m}$ )	$5.19 \pm 0.22$	$7.02 \pm 0.17$	$6.86 \pm 0.10$	$-0.77 \pm 0.41$	$-11.0 \pm 5.8$	0.0712
$l$ ( $\mu\text{m}$ )	$22.9 \pm 0.54$	$28.6 \pm 1.96$	$39.0 \pm 2.17$	$9.93 \pm 2.56$	$34.7 \pm 9.0$	0.0006
$C$ (cells/ $10^3 \mu\text{m}^2$ )	$9.08 \pm 1.01$	$5.42 \pm 0.31$	$3.22 \pm 0.31$	$-1.20 \pm 0.57$	$-22.1 \pm 10.5$	0.0341

measurements of the flow speed, a *V. carteri* spheroid was caught such that the micropipette aspiration point was approximately on the equator. The micropipette was then rotated until the *Volvox* anterior–posterior axis was in the focal plane. The flow speed was read out at the *Volvox* equator on the side opposite the aspiration point, just above the spheroid surface (10  $\mu\text{m}$  above the flagellar tips), as the flow speed reaches a maximum there. This maximum speed  $U$  can be related mathematically to the force the flagella generate [5]. Flagellar beating frequencies were determined by averaging across 10 beating periods, and averaging across five somatic cells around the *Volvox* equator. The experiment was repeated four times, yielding data on  $n=80$  *V. carteri* colonies between the two nutrient treatments.

For each *Volvox* colony, the measured peak fluid speed  $U$  was used to estimate the total force  $F$  that all flagella exert on the fluid. Using a mathematical model, Short *et al.* [5] found that  $F=64\eta RU/3$ , where  $R$  is the *Volvox* radius and  $\eta$  is the viscosity of water. Taking into account that the flagellar force is applied to the fluid from the surface of a sphere, the net forward thrust can be shown to be  $F_p = \pi F/4$  [26]. The measured colony, somatic and germ cell radii, and the calculated  $F_p$ , were then used to estimate the upward swimming speed  $V_{\text{up}}$  for each colony. As described in detail in Solari *et al.* [8],  $V_{\text{up}} = (F_p - g\Delta M)/6\pi\eta R$ , where  $g$  is the acceleration of gravity and  $\Delta M$  is the difference in mass between the cells and the displaced water, assuming that the ECM

is approximately neutrally buoyant (measured cell densities were taken from [27]).

### 3. RESULTS AND DISCUSSION

Table 1 gives results from the initial experiments on phenotypic differences in populations that were grown in normal and diluted media, at a light intensity of 1000 fc. Table 2 contains the results from the more detailed experiments on *V. carteri*, in which populations were grown at 600 fc. It also contains the swimming and sedimentation speeds, as well as the thrust force calculations of *C. reinhardtii* and *G. pectorale*. Figure 4 illustrates the effects of the nutrient deprivation on *V. carteri*. Details of the MLR models that were used to quantify phenotypic alterations are given in tables 3 and 4.

For *C. reinhardtii* and *G. pectorale*, the only evident phenotypic alteration was that cells grown in diluted medium were smaller than those grown in normal medium (table 1); there was no difference in flagellar length between treatments. This reduction in cell size upon nutrient deprivation is not surprising, as nutrient uptake in these organisms is dominated by diffusion (the relevant Péclet number is  $Pe \sim 0.1$ ), implying that *C. reinhardtii* and *G. pectorale* can take no measures to oppose starvation if the growth medium is low in nutrients. The swimming and sedimentation speeds and swimming force calculations confirm these

Table 2. Data from *C. reinhardtii*, *G. pectorale* and *V. carteri* populations grown at a light intensity of 600 fc, i.e. experiments described in §§2.2 and 2.3. The format and notation are as in table 1. Additional symbols are the flagellar beating frequency  $f$ , the peak flow speed at the equator  $U$  (described in §2), the net force that all flagella exert on the fluid  $F$ , the propulsion force  $F_p$ , the upward swimming speed  $V_{up}$  and the sedimentation speed  $V_{sed}$ . For each measurement on *V. carteri*,  $n = 40$  colonies were used. For measurements on *C. reinhardtii* and *G. pectorale*,  $n = 120$  individuals were used for  $V_{up}$  and  $V_{sed}$ , and  $n = 4$  populations for  $F_p$ . Details of the MLR model used here are given in table 4. The average number of somatic cells of a *V. carteri* colony was  $1557 \pm 50$ , and the average number of germ cells was  $10.0 \pm 0.2$ . In these experiments, the average number of cells in *G. pectorale* colonies was  $4.1 \pm 0.19$ .

	$t_2$ : normal medium	$t_2$ : diluted medium	difference between treatments		
			absolute	(%)	$p$ -value
<i>C. reinhardtii</i>					
$V_{sed}$ ( $\mu\text{m s}^{-1}$ )	$6.5 \pm 0.24$	$3.7 \pm 0.14$	$-2.75 \pm 0.27$	$-42.3 \pm 4.2$	$<0.0001$
$V_{up}$ ( $\mu\text{m s}^{-1}$ )	$43 \pm 1.9$	$54 \pm 2.6$	$11.41 \pm 3.32$	$26.5 \pm 7.7$	0.0007
$F_p$ (pN)	$5.59 \pm 0.57$	$5.13 \pm 0.39$	§	§	0.5367
<i>G. pectorale</i>					
$V_{sed}$ ( $\mu\text{m s}^{-1}$ )	$10.0 \pm 0.39$	$8.9 \pm 0.37$	$-1.11 \pm 0.54$	$-11.1 \pm 5.4$	0.0400
$V_{up}$ ( $\mu\text{m s}^{-1}$ )	$33 \pm 1.3$	$37 \pm 1.1$	$4.21 \pm 1.76$	$12.8 \pm 5.3$	0.0176
$F_p$ (pN)	$8.89 \pm 0.93$	$9.06 \pm 0.60$	§	§	0.8847
<i>V. carteri</i>					
$R$ ( $\mu\text{m}$ )	$144 \pm 3.5$	$174 \pm 3.9$	$27.2 \pm 3.32$	$18.9 \pm 2.3$	$<0.0001$
$r_G$ ( $\mu\text{m}$ )	$26.7 \pm 0.56$	$27.1 \pm 0.53$	§	§	0.6384
$r_S$ ( $\mu\text{m}$ )	$4.63 \pm 0.06$	$4.40 \pm 0.05$	$-0.25 \pm 0.07$	$-5.4 \pm 1.5$	$<0.0001$
$l$ ( $\mu\text{m}$ )	$17.49 \pm 0.19$	$19.49 \pm 0.26$	$0.93 \pm 0.25$	$5.3 \pm 1.4$	$<0.0001$
$C$ (cells/ $10^3 \mu\text{m}^2$ )	$8.93 \pm 0.44$	$6.21 \pm 0.29$	$-2.57 \pm 0.34$	$-28.8 \pm 4.0$	$<0.0001$
$f$ (Hz)	$27.4 \pm 0.27$	$26.3 \pm 0.36$	$0.66 \pm 0.45$	$2.4 \pm 1.6$	0.1521
$U$ ( $\mu\text{m s}^{-1}$ )	$436 \pm 11.2$	$435 \pm 9.5$	§	§	0.4232
$F$ (pN)	$1932 \pm 63.6$	$2157 \pm 55.4$	$211 \pm 51$	$10.9 \pm 2.6$	$<0.0001$
$V_{up}$ ( $\mu\text{m s}^{-1}$ )	$274 \pm 14.5$	$300 \pm 12.3$	$26 \pm 14.4$	$9.5 \pm 5.3$	0.0718

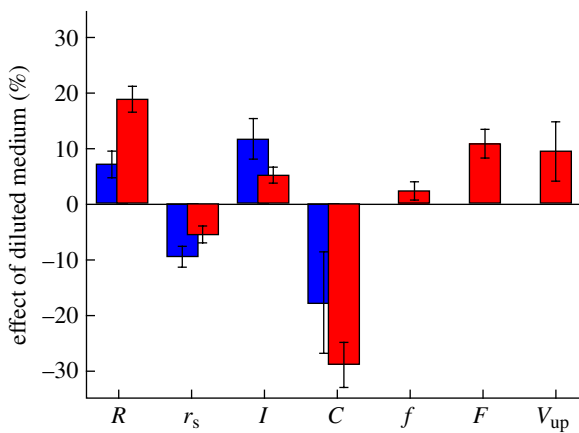


Figure 4. Bar chart showing the percentage changes of properties of *V. carteri* colonies grown in diluted medium, with respect to those grown in normal medium. The two colours indicate results from the different experiments: table 1 in blue (1000 fc), and table 2 in red (600 fc). Error bars show the standard error. The symbols used are the spheroid radius  $R$ , somatic cell radius  $r_s$ , flagellar length  $l$ , somatic cell concentration  $C$ , flagellar frequency  $f$ , net force of flagella on the fluid  $F$ , and the upward swimming speed  $V_{up}$ .

results: *C. reinhardtii* and *G. pectorale* have significantly higher swimming speeds and lower sedimentation speeds in diluted media owing to the decrease in cell size, but there is no difference in propulsion force between the treatments.

In contrast, *V. carteri* and *V. barberi* displayed intriguing phenotypic changes when grown for a short

period in a low-nutrient medium. Regardless of treatment, *V. barberi* has a higher cell concentration per unit area and longer flagella than *V. carteri* (table 1). The initial experiments (table 1) showed that colonies grown in diluted media had smaller somatic cells with longer flagella and larger spheroids for both species, the latter owing to an increased amount of ECM. We investigated in more detail the phenotypic alterations of *V. carteri* (table 2), by using equipment that allowed measurements of the peak fluid speed  $U$ , the flagellar beating frequency  $f$  and the force exerted by the flagella on the fluid  $F$ . Because in these more detailed experiments colonies were grown with lower light intensity (approx. 600 fc instead of approx. 1000 fc), they had fewer cells, and reached a smaller spheroid, cell and flagellar size than in the initial experiments. However, the data from the more detailed experiments had a better statistical significance and qualitatively confirm the results from the initial experiments (see comparison in figure 4). It is worth noting that these experiments showed that, regardless of nutrient treatment, colonies with lower cell concentration have longer flagella, and that colonies with longer flagella have a lower beating frequency (table 4). Further, results from these more detailed experiments showed that there was no difference in fluid speed  $U$  between treatments, even though the biflagellated somatic cells were more sparsely spaced in the diluted medium owing to the larger spheroid size under those conditions. As there is only very weak evidence for a small increase in flagellar beating frequency upon dilution (table 2), the fact that the flow speed  $U$  remains constant despite

Table 3. Model results for the MLR analysis of experiments conducted with populations grown at a light intensity of 1000 fc, i.e. experiment described in §2.1. The notation is as in table 1. Additional symbols are the total number of flagellated cells in colonies  $N_S$ , the change  $\Delta$  of the measured quantity over 8 h in normal medium and  $\Delta + \delta$  in diluted medium. Data analysis takes the form  $d = d_0 + \sum_i a_i v_i + \sum_i b_i N_{S,i}$ , with dummy indicator variables  $v_i = 0, 1$  to take account of nominal factors such as the medium treatment, and  $a, b$  and  $d_0$  are parameters of the model. A § marks statistically non-significant terms. Differences between replicated experiments were taken into account as a nominal factor and are not reported. In *G. pectorale*, we found that colonies with more cells had smaller cells with longer flagella regardless of treatment. In *Volvox*, we found that colonies with a larger number of flagellated cells  $N_S$  had a larger radius  $R$  and a larger cell concentration per unit area  $C$ . In *V. barberi* colonies with more cells, somatic cells were smaller. Because *V. barberi* germ cells perform binary fission, it was not possible to measure the germ cell size accurately.

	$d_0$	$\Delta$	$\delta$	$N_S$	$r^2$	$F$ -ratio
<i>C. reinhardtii</i>						
$r_C$ ( $\mu\text{m}$ )	$3.43 \pm 0.12$	$1.46 \pm 0.18$	$-0.36 \pm 0.18$	—	0.58	29
$l$ ( $\mu\text{m}$ )	$10.18 \pm 0.28$	$-1.50 \pm 0.39$	§	—	0.43	16
<i>G. pectorale</i>						
$r_C$ ( $\mu\text{m}$ )	$5.58 \pm 0.44$	$0.82 \pm 0.25$	$-0.34 \pm 0.16$	$-0.14 \pm 0.06$	0.45	21
$l$ ( $\mu\text{m}$ )	§	§	§	$0.57 \pm 0.25$	0.17	5
<i>V. carteri</i>						
$R$ ( $\mu\text{m}$ )	$126 \pm 8.1$	$46 \pm 5.4$	$14.6 \pm 4.86$	$0.013 \pm 0.003$	0.65	41
$r_G$ ( $\mu\text{m}$ )	$23.2 \pm 0.53$	$6.1 \pm 0.70$	$-1.16 \pm 0.63$	§	0.53	29
$r_S$ ( $\mu\text{m}$ )	$3.81 \pm 0.08$	$0.79 \pm 0.10$	$-0.46 \pm 0.09$	§	0.58	34
$l$ ( $\mu\text{m}$ )	$14.28 \pm 0.58$	$3.03 \pm 0.77$	$2.14 \pm 0.68$	§	0.48	23
$C$ (cells/ $10^3 \mu\text{m}^2$ )	$3.07 \pm 0.56$	$-2.88 \pm 0.37$	$-0.65 \pm 0.33$	$0.021 \pm 0.0002$	0.69	48
<i>V. barberi</i>						
$R$ ( $\mu\text{m}$ )	$170 \pm 15.0$	$60 \pm 10.5$	$59.1 \pm 11.0$	$0.009 \pm 0.002$	0.82	74
$r_S$ ( $\mu\text{m}$ )	$6.11 \pm 0.28$	$1.88 \pm 0.20$	$-0.39 \pm 0.21$	$-0.0003 \pm 0.0001$	0.82	109
$l$ ( $\mu\text{m}$ )	$24.80 \pm 3.51$	$5.80 \pm 2.46$	$9.93 \pm 2.56$	§	0.63	22
$C$ (cells/ $10^3 \mu\text{m}^2$ )	$4.99 \pm 0.93$	$-3.85 \pm 0.65$	$-1.20 \pm 0.57$	$0.0008 \pm 0.0002$	0.81	65

Table 4. Model results for the MLR analysis (as explained in table 3) of experiments described in §§2.2 and 2.3 conducted with populations of *V. carteri*, *C. reinhardtii* and *G. pectorale* grown at a light intensity of 600 fc. The notation is as in table 3. For *V. carteri*, the continuous variable  $T$  ranges from 1 to 4 to account for the four intervals of 30 min where data were recorded. A § marks statistically non-significant terms. As in the previous analysis, an increase in  $N_S$  increases  $R$  and  $C$ . Moreover, we found that colonies with more cells had smaller  $r_S$ , larger  $U$  and larger  $F$ . In the 2 h measurement window, the colony spheroid, germ cells and flagella continued growing and the cell concentration continued decreasing significantly with time. Interestingly, the flagellar length  $l$  was significantly smaller when the cell concentration was large, regardless of treatment. The flagellar beating frequency  $f$  was found to be lower when the flagellar length was larger.

	$d_0$	$\delta$	$N_S$ ( $10^{-3}$ )	$T$	$C$	$l$	$r^2$	$F$ -ratio
<i>C. reinhardtii</i>								
$r_C$ ( $\mu\text{m}$ )	$5.90 \pm 0.11$	$-1.25 \pm 0.16$	—	—	—	—	0.42	19
$V_{\text{sed}}$ ( $\mu\text{m s}^{-1}$ )	$7.18 \pm 0.35$	$-2.75 \pm 0.27$	—	—	—	—	0.32	56
$V_{\text{up}}$ ( $\mu\text{m s}^{-1}$ )	$42.8 \pm 2.45$	$11.41 \pm 3.32$	—	—	—	—	0.05	12
<i>G. pectorale</i>								
$r_C$ ( $\mu\text{m}$ )	$6.61 \pm 0.18$	$-0.31 \pm 0.14$	$-220 \pm 30$	—	—	—	0.31	11
$V_{\text{sed}}$ ( $\mu\text{m s}^{-1}$ )	$11.0 \pm 0.39$	$-1.11 \pm 0.54$	§	—	—	—	0.02	4
$V_{\text{up}}$ ( $\mu\text{m s}^{-1}$ )	$32.5 \pm 1.35$	$4.21 \pm 1.76$	§	—	—	—	0.02	6
<i>V. carteri</i>								
$R$ ( $\mu\text{m}$ )	$112 \pm 7.6$	$27.2 \pm 3.32$	$16 \pm 4$	$5.29 \pm 1.49$	—	—	0.75	37
$r_G$ ( $\mu\text{m}$ )	$26.0 \pm 0.70$	§	§	$0.40 \pm 0.26$	—	—	0.35	10
$r_S$ ( $\mu\text{m}$ )	$5.13 \pm 0.14$	$-0.25 \pm 0.07$	$-0.27 \pm 0.09$	§	—	—	0.41	10
$l$ ( $\mu\text{m}$ )	$19.18 \pm 0.59$	$0.93 \pm 0.25$	§	$0.44 \pm 0.10$	$-0.32 \pm 0.05$	—	0.67	25
$C$ (cells per $10^3 \mu\text{m}^2$ )	$4.23 \pm 0.77$	$-2.57 \pm 0.34$	$4 \pm 0.4$	$-0.48 \pm 0.15$	—	—	0.70	29
$f$ (Hz)	$39.3 \pm 2.45$	$0.66 \pm 0.45$	§	§	—	$-0.70 \pm 0.14$	0.26	13
$U$ ( $\mu\text{m s}^{-1}$ )	$368 \pm 21$	§	$68 \pm 11$	$-10.1 \pm 4.23$	—	—	0.58	20
$F$ (pN)	$1249 \pm 105$	$211 \pm 51$	$443 \pm 64$	§	—	—	0.68	31
$V_{\text{up}}$ ( $\mu\text{m s}^{-1}$ )	$274 \pm 10.2$	$26 \pm 14.4$	§	§	—	—	0.46	16

the increased cell separation implies that the increase in flagellar length provides the necessarily increased beating force  $F$ . Also, weak evidence from the detailed

experiments on *V. carteri* suggests that the upward swimming speed (estimated  $V_{\text{up}}$ ) increased for colonies grown in the diluted medium (table 2 and figure 4). In

the diluted medium, colonies have smaller somatic cells (i.e. lower negative gravitational force) and longer flagella (i.e. larger swimming force). These benefits seem to outweigh the increase in drag owing to the larger spheroid of colonies grown in diluted medium.

A plausible interpretation of the results showing that *Volvox* colonies, when grown in a diluted medium, make investments into collective properties, such as a larger spheroid radius  $R$  and maintaining a high fluid speed  $U$ , is that these changes tend to increase the rate of nutrient uptake and thereby help compensate for the environmental change. There are two key physical aspects that must be considered in estimating the rate of nutrient uptake to a spherical organism like *Volvox*. The first is the fact that the absorbing somatic cells cover only a fraction of the total colony surface, and it is not obvious *a priori* how even the purely diffusive rate of uptake would depend on the somatic cell size and the overall colony radius in a geometry with such patchy absorbers. However, this is precisely the problem considered some time ago in the context of chemoreception [28]. There it was found that the absorption rate  $J$  to a sphere of radius  $R$  whose surface is covered by  $n$  absorbing discs, each of radius  $r_S$ , is  $J_{\max} nr_S / (nr_S + \pi R)$ , where  $J_{\max} = 4\pi DC_{\infty} R$  is the rate associated with a sphere whose *entire* surface is a perfect absorber. When the number of discs tends to infinity the rate sensibly approaches  $J_{\max}$ , but the key point is that it can be very close to this asymptotic value even for moderate coverage of the surface. (The first detailed discussion of this kind of effect was given by Jeffreys [29] in the context of evaporation from the stomata on leaves.) Expressing the result as  $J = 4\pi DC_{\infty} R / (1 + \pi R / nr_S)$ , and using the values typical of *Volvox* ( $n = 1000$ ,  $R = 250 \mu\text{m}$ ,  $r_S = 5 \mu\text{m}$ ), the ratio  $\pi R / nr_S \sim 0.16$  and thus  $J / J_{\max} = 0.86$ , only slightly depressed from the asymptotic value. We conclude from this that the surface coverage of somatic cells in *Volvox* is sufficiently large that not only is the diffusive rate of absorption well approximated by that of a sphere absorbing over its entire surface, but even quite substantial increases in the colony radius still leave it in that regime, so the *purely diffusive absorption rate actually increases with colony radius at fixed somatic cell number*. This would not be the case for very small  $nr_S$  ( $\pi R / nr_S \gg 1$ ), for then the rate is simply proportional to  $nr_S$  and independent of the colony radius  $R$ . Using the typical values of  $R$  and  $r_S$  above, this would require  $n \ll 150$ .

The second issue to consider is how the presence of a fluid flow past the colony surface might affect the results described above. While there has been no detailed mathematical analysis of this particular problem, we may draw some conclusions based on the typical flow rates and diffusivities. The key physical feature that results in the diffusive flux in the absence of flow being so close to the fully absorbing sphere value is the very large number of encounters that a diffusing molecule makes with the sphere when it is in the vicinity of the surface [28]. It follows then that advection *parallel* to the surface would not significantly alter this effect (in fact it may even enhance it) provided the time spent near the surface during advection is

not severely curtailed. In the case of *Volvox* the time scale for advection along the colony surface is several seconds, and in that time a molecule would typically diffuse a distance  $(2Dt)^{1/2} \sim 40 \mu\text{m}$ , a distance large compared with the somatic cell size and comparable to if not greater than the intersomatic cell spacing. Thus, as the molecules are swept over the surface, they indeed have sufficient time to find an absorbing somatic cell.

The arguments advanced above suggest that nutrient uptake for an organism like *Volvox* can be estimated on the basis of a fully absorbing sphere. Attention then turns to the rate of uptake at high Péclet numbers. For a *Volvox* spheroid,  $Pe = 2RU/D$ , as the typical length scale over which the self-generated flow changes is  $2R$  [5]. Increasing  $R$  and maintaining a high  $U$  may thus be seen as a strategy for *Volvox* to maintain, or even increase, the high  $Pe$ . Such a strategy is beneficial for the colony, as the rate of nutrient uptake by a ciliated spherical micro-organism through its surface is predicted to be proportional to  $R Pe^{1/2}$  [5,30]. Qualitatively, this  $Pe$  dependence of the nutrient uptake rate can be understood by noting that the high flow speeds create a fluid-dynamical boundary layer above the spheroid surface across which there is a steep nutrient concentration gradient, which leads to an enhanced diffusive transport across the boundary layer onto the organism surface. This strong dependence on Péclet number for large organisms should be contrasted with that for small organisms. A variety of calculations [5,30] suggest that, for organisms with a small Péclet number, the correction to the diffusive uptake owing to fluid flow is linear in  $Pe$ . Thus, an organism in the regime  $Pe < 1$  will in general make only a small change to its uptake rate by a fractional change in  $Pe$ , whereas a comparable change in  $Pe$  for  $Pe \gg 1$  can produce a much larger change in uptake, proportional to  $Pe^{1/2}$ . Even though *Volvox* is a colonial organism without a central nervous system, the phenotypic plasticity it displays suggests ‘awareness’ of the benefits associated with collective behaviour. The self-generated fluid flows are thus not only important for self-propulsion and phototaxis [31], but also for nutrient uptake.

The efforts of *Volvox* to counteract an impending decrease in nutrient uptake, if grown in low-nutrient medium, have a positive effect on the growth of the germ cells (which later turn into the daughter colonies; figure 3) in *V. carteri*. In the initial experiments, there was statistically weak evidence for a small dependence of the germ cell radii  $r_G$  on the nutrient treatment (table 1), but there was no statistically significant dependence of  $r_G$  on the nutrient treatment in the more detailed experiments (table 2). These results suggest that, in the investigated time window of the *Volvox* life cycle, colonies can maintain (almost) equal germ cell growth rates in normal and  $10^{-1}$  diluted media.

#### 4. CONCLUSION

We found evidence that growth in low-nutrient medium induces phenotypic plasticity that mitigates the effect of nutrient limitation in large Volvocales (*V. carteri*



and *V. barberi*), and a lack of such plasticity in small Volvocales (*C. reinhardtii* and *G. pectorale*). The changes in phenotype induced by growing *Volvox* in a diluted medium were investments into advective fluid flows, and into an increase in colony radius. Such investments point to the important role of advection in enhancing nutrient uptake for the germ cells that grow inside the *Volvox* colony, consistent with recent theory [5] and experiments [16] which suggested a link between the Péclet number and the evolution to larger organism sizes and germ–soma differentiation in the Volvocales. Although this work provides further evidence for the importance of advection in nutrient uptake for large multicellular micro-organisms, direct measurement of the advection dependence of the rate of nutrient uptake or metabolic activity still require further study. Likewise, further studies are needed to understand the control of collective flagellar beating and the connection between flagellar beating frequency, length and spacing.

We are grateful to Matt Herron for a critical reading of the manuscript and many detailed suggestions, and thank J.-W. van de Meent, T. J. Pedley and I. Tuval for discussions. This work was supported in part by NSF grants DEB-0075296 (C.A.S., R.E.M.) and PHY-0551742 (S.G., J.O.K., R.E.G.), the Engineering and Biological Systems programme of the BBSRC and the Schlumberger Chair Fund.

## REFERENCES

- Grosberg, R. K. & Strathmann, R. R. 2007 The evolution of multicellularity: a minor mayor transition? *Annu. Rev. Ecol. Evol. Syst.* **38**, 621–654. (doi:10.1146/annurev.ecolsys.36.102403.114735)
- Smith, J. M. & Szathmáry, E. 1995 *The major transitions in evolution*. Oxford, UK: Oxford University Press.
- Niklas, K. J. 1994 *Plant allometry*. Chicago, IL: University of Chicago Press.
- Weismann, A. 1891 *Essays upon heredity and kindred biological problems*. Oxford, UK: Clarendon Press.
- Short, M. B., Solari, C. A., Ganguly, S., Powers, T. R., Kessler, J. O. & Goldstein, R. E. 2006 Flows driven by flagella of multicellular organisms enhance long-range molecular transport. *Proc. Natl Acad. Sci. USA* **103**, 8315–8319. (doi:10.1073/pnas.0600566103)
- Kirk, D. L. 1998 *Volvox: molecular-genetic origins of multicellularity and cellular differentiation*. Cambridge, UK: Cambridge University Press.
- Koufopanou, V. 1994 The evolution of soma in the Volvocales. *Am. Nat.* **143**, 907–931. (doi:10.1086/285639)
- Solari, C. A., Kessler, J. O. & Michod, R. E. 2006 A hydrodynamics approach to the evolution of multicellularity: flagellar motility and the evolution of germ–soma differentiation in volvocalean green algae. *Am. Nat.* **167**, 537–554. (doi:10.1086/501031)
- Coleman, A. W. 1999 Phylogenetic analysis of ‘Volvocaceae’ for comparative genetic studies. *Proc. Natl Acad. Sci. USA* **96**, 13 892–13 897. (doi:10.1073/pnas.96.24.13892)
- Herron, M. D. & Michod, R. E. 2008 Evolution of complexity in the volvocine algae: transitions in individuality through Darwin’s eye. *Evolution* **62**, 436–451. (doi:10.1111/j.1558-5646.2007.00304.x)
- Nozaki, H., Ohta, N., Takano, H. & Watanabe, M. M. 1999 Reexamination of phylogenetic relationships within the colonial Volvocales (Chlorophyta): an analysis of atpB and rbcL gene sequences. *J. Phycol.* **35**, 104–112. (doi:10.1046/j.1529-8817.1999.3510104.x)
- Nozaki, H. 2003 Origin and evolution of the genera *Pleodorina* and *Volvox* (Volvocales). *Biologia* **58**, 425–431.
- Nozaki, H., Ott, F. D. & Coleman, A. W. 2006 Morphology, molecular phylogeny and taxonomy of two new species of *Pleodorina* (Volvocaceae, Chlorophyceae). *J. Phycol.* **42**, 1072–1080. (doi:10.1111/j.1529-8817.2006.00255.x)
- Larson, A., Kirk, M. M. & Kirk, D. L. 1992 Molecular phylogeny of the volvocine flagellates. *Mol. Biol. Evol.* **9**, 85–105.
- Reynolds, C. S. 1984 *The ecology of freshwater phytoplankton*. Cambridge, UK: Cambridge University Press.
- Solari, C. A., Ganguly, S., Kessler, J. O., Michod, R. E. & Goldstein, R. E. 2006 Multicellularity and the functional interdependence of motility and molecular transport. *Proc. Natl Acad. Sci. USA* **103**, 1353–1358. (doi:10.1073/pnas.0503810103)
- Hoops, H. J. 1997 Motility in the colonial and multicellular Volvocales: structure, function, and evolution. *Protoplasma* **199**, 99–112. (doi:10.1007/BF01294499)
- Guyon, E., Hulin, J. P., Petit, L. & Mitescu, C. D. 2001 *Physical hydrodynamics*. New York, NY: Oxford University Press.
- Purcell, E. M. 1977 Life at low Reynolds number. *Am. J. Phys.* **45**, 3–11. (doi:10.1119/1.10903)
- Sultan, S. E. 2000 Phenotypic plasticity for plant development, function and life history. *Trends Plant Sci.* **5**, 537–542. (doi:10.1016/51360-1385(00)01797-0)
- Miner, B. G. 2005 Evolution of feeding structure plasticity in marine invertebrate larvae: a possible trade-off between arm length and stomach size. *J. Exp. Mar. Biol. Ecol.* **315**, 117–125. (doi:10.1016/j.jembe.2004.09.011)
- Kirk, D. L. & Kirk, M. M. 1983 Protein synthetic patterns during the asexual life cycle of *Volvox carteri*. *Dev. Biol.* **96**, 493–506. (doi:10.1016/0012-1606(83)90186-0)
- Desnitski, A. G. 1995 A review on the evolution of development in *Volvox*: morphological and physiological aspects. *Eur. J. Protistol.* **31**, 241–247.
- Solari, C. A., Michod, R. E. & Goldstein, R. E. 2008 *Volvox barberi*, the fastest swimmer of the Volvocales (Chlorophyceae). *J. Phycol.* **44**, 1395–1398. (doi:10.1111/j.1529-8817.2008.00603.x)
- Drescher, K., Leptos, K. C. & Goldstein, R. E. 2009 How to track protists in three dimensions. *Rev. Sci. Instrum.* **80**, 014301. (doi:10.1063/1.3053242)
- Drescher, K., Leptos, K. C., Tuval, I., Ishikawa, T., Pedley, T. J. & Goldstein, R. E. 2009 Dancing *Volvox*: hydrodynamic bound states of swimming algae. *Phys. Rev. Lett.* **102**, 168101. (doi:10.1103/PhysRevLett.102.168101)
- Solari, C. A. 2005 A hydrodynamics approach to the evolution of multicellularity: flagellar motility and the evolution of germ–soma differentiation in volvocalean green algae. PhD thesis, University of Arizona, USA.
- Berg, H. C. & Purcell, E. M. 1977 Physics of chemoreception. *Biophys. J.* **20**, 193–219. (doi:10.1016/S0006-3495(77)85544-6)
- Jeffreys, H. 1918 Some problems of evaporation. *Phil. Mag.* **35**, 423–441.
- Magar, V., Goto, T. & Pedley, T. J. 2003 Nutrient uptake by a self-propelled steady squirmer. *Q. J. Mechanics Appl. Math.* **56**, 65–91. (doi:10.1093/qjmath/56.1.65)
- Drescher, K., Goldstein, R. E. & Tuval, I. 2010 Fidelity of adaptive phototaxis. *Proc. Natl Acad. Sci. USA* **107**, 11 171–11 176. (doi:10.1073/pnas.1000901107)